Monitoring the Daily Evolution and Extent of Snow Drought

Benjamin J. Hatchett[1], Alan M. Rhoades[2], and Daniel J. McEvoy[1]

[1]Desert Research Institute, Reno, Nevada, USA, 89512
[2]Climate and Ecosystem Sciences Division, Lawrence Berkeley National Laboratory, Berkeley, California, USA, 94720

Correspondence: Benjamin J. Hatchett (benjamin.hatchett@gmail.com)

Abstract. Snow droughts are commonly defined as below average snowpack at a point in time, typically 1 April in the western United States (wUS). This definition is valuable for interpreting the state of the snowpack but obscures the temporal evolution of snow drought. Borrowing from dynamical systems theory, we applied phase diagrams to visually examine the evolution of snow water equivalent (SWE) and accumulated precipitation conditions in maritime, intermountain, and continental snow climates in the wUS using station observations as well as spatially distributed estimates of SWE and precipitation. Using a percentile-based drought definition phase diagrams of daily observed SWE and precipitation highlighted decision-relevant aspects of snow drought such as onset, evolution, and termination. The phase diagram approach can be used in tandem with spatially distributed estimates of daily SWE and precipitation to reveal variability in snow drought type and extent. When combined streamflow or other data, phase diagrams and spatial estimates of snow drought conditions can help inform drought monitoring and early warning and help link snow drought type and evolution impacts on ecosystems, water resources, and recreation. A web tool is introduced allowing users to create real-time or historic snow drought phase diagrams.

1 Introduction

Snow-dominated mountains provide critical water resources to ecosystems and society (Viviroli et al., 2007; Sturm et al., 2017; Immerzeel et al., 2020), but their snowpacks are susceptible to climate warming (Beniston, 2003; Pepin et al., 2015; Rhoades et al., 2018c; Siirila-Woodburn et al., 2021). Warming impacts mountain regions in many ways, including reductions in the amount of water stored in snowpack (Mote et al., 2018), earlier spring snowmelt (Kapnick and Hall, 2012; Musselman et al., 2021), and slower snowmelt (Musselman et al., 2017). Warming increases the frequency of extreme rain-on-snow events (Musselman et al., 2018) and generally decreases the fraction of precipitation falling as snow (Lynn et al., 2020). As rain falls instead of snow, runoff becomes less efficient (Berghuijs et al., 2014), a process amplified by increasing atmospheric demand for moisture (Fisher et al., 2017).

Spring snowpack is an important predictor of warm season runoff for environmental flows and human consumptive use. Projected snowpack losses in upwards of 89% of areas western United States (wUS) historically characterized by a seasonal snowpack by end-century will reduce drought prediction skill in these regions (Livneh and Badger, 2020). Losses will be pronounced in lower elevation coastal snowpacks that are most "at risk" to warming (Nolin and Daly, 2006; Dierauer et al., 2019; Hatchett, 2021; Evan and Eisenman, 2021). In addition to downstream agricultural (Qin et al., 2020), environmental (Poff et al., 1997; Yarnell et al., 2020) and other economic impacts (Lund et al., 2018; Sturm et al., 2017), reductions in snowpack

negatively impact wildlife habitat (Barsugli et al., 2020) and decrease opportunities for recreation and tourism (Scott, 2006; Hatchett and Eisen, 2019; Crowley et al., 2019). In many rural mountain regions, recreation and tourism are pillars of the economy (Hagenstad et al., 2018).

30   Tracking snowpack throughout the wUS cool season (defined broadly as November-May) and identifying below-normal snow conditions known as "snow drought" (Cooper et al., 2016; Harpold et al., 2017; Hatchett and McEvoy, 2018; Huning and AghaKouchak, 2020a) aids resource managers in making decisions (e.g., water allocations) based on the state of the snowpack relative to past and forecast conditions and forecast snowpack conditions. Often, a point-in-time approach is used to assess snowpack conditions pertaining to runoff. For example, the date of 1 April is codified into many wUS water management
35   agencies (Lynn et al., 2020) that depend on runoff from both seasonal and ephemeral snowpacks (Hatchett, 2021) to assess warm season water availability. The relation of this date to peak snowpack timing and its representatives of the total volume of potential meltwater, however, varies by location and season (Trujillo and Molotch, 2014; Margulis et al., 2019; Musselman et al., 2021; Siirila-Woodburn et al., 2021). Hatchett and McEvoy (2018) highlight other challenges of the single point-in-time definition. Notably, they discussed that pre-1 April snow droughts can be obscured by later heavy snowfall and that anomalous
40   melt events during warmer-than-normal conditions can create snow drought conditions not directly related to precipitation.

    These challenges, and the need to communicate mountain hydroclimate conditions varied user groups (e.g., the National Weather Service, natural resource managers and other decision makers (Marshall et al., 2020)), illustrate the need for easily-accessible, informative data visualization approaches that capture the signals of interest for decision-relevant contexts and allows a user to track their evolution through the water year (WY). Here, we introduce the application of phase diagrams which
45   enable the visualization of how two variables co-vary through time. Specifically, we show the daily temporal co-evolution of snow water equivalent (SWE) and precipitation. We also demonstrate the utility of this approach using examples across a range of spatial scales in wUS snow-dominated regions. We also highlight intraseasonal and interannual snowpack variability, snow drought variation along an elevational and longitudinal transect, and how dry snow droughts (below-average precipitation and snowpack) versus warm snow droughts (above-average precipitation but below-average snowpack) differ. Last, a web-based
50   tool enabling the creation of phase diagrams "in real time" based on the SNOTEL network is introduced: https://wrcc.dri.edu/my/climate/snow-drought-tracker.

2   Data

2.1   Station Observations

Daily observations of SWE and accumulated WY precipitation (the WY begins on 1 October and ends on 30 September,
55   with the year corresponding to the latter date) were acquired from seven SNOwpack TELemetry (SNOTEL) stations from the Natural Resources Conservation Survey (https://www.wcc.nrcs.usda.gov/snow/) across the wUS (Figure 1; 1). SNOTEL is a long-term, quality-controlled, surface-based network for observing precipitation and snow in wUS mountains (Serreze et al., 1999). We used SNOTEL stations located in California, Colorado, Nevada, Utah, and Washington. These stations exemplify a range of snow climates (maritime, intermountain, and continental). We acquired daily SNOTEL data spanning the period of

60 record (typically beginning in the 1980s) through 31 May, 2020 for complete WYs. In our example highlighting the web-based
tool, we used an end date of 8 March, 2021 to show the real-time application of phase diagrams. Last, we acquired daily
streamflow for WYs 1943–2019 from the U.S. Geological Survey Gage 12082500, located on the unimpaired Nisqually River,
near the Paradise, Washington SNOTEL site (1b) to show how to link phase diagrams with hydrologic outcomes.
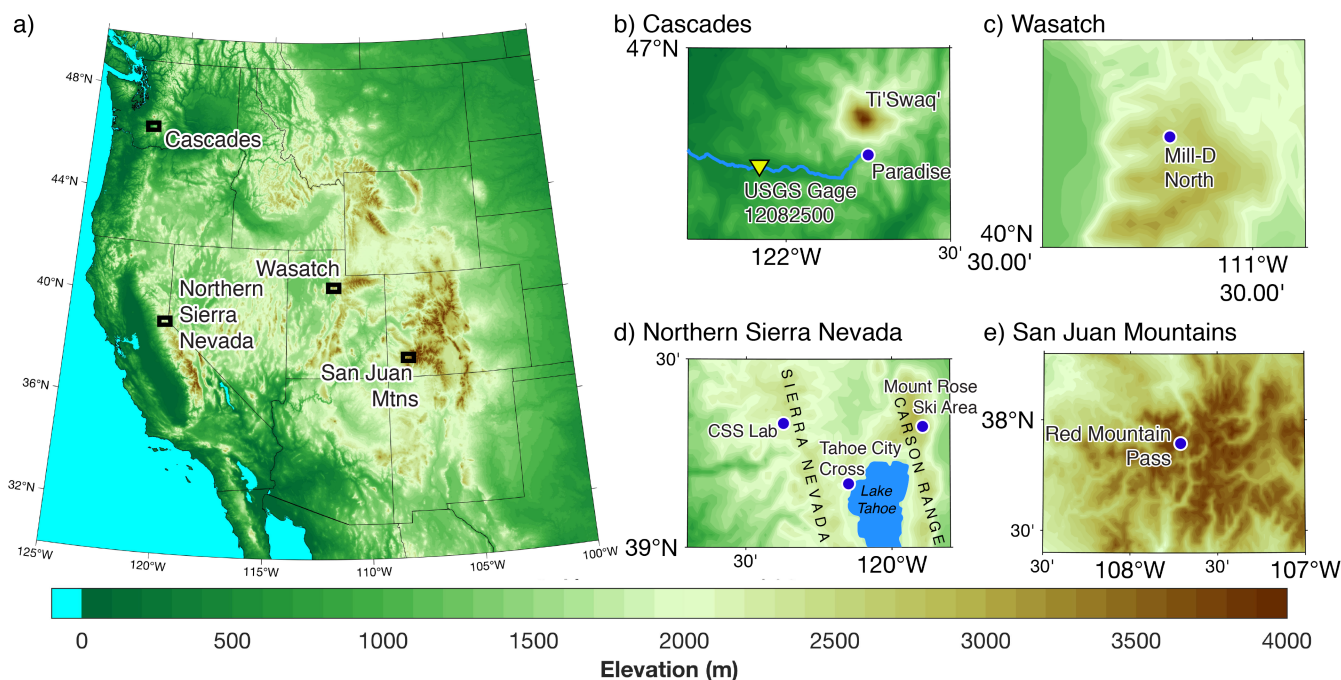
Figure 1. (a) Digital elevation map of western United States topography (in m) from ETOPO (Amante and Eakins, 2009) showing study
areas of focus: **(b)** the Cascade Mountains, **(c)** the Wasatch Mountains, **(d)** the Northern Sierra Nevada, and **(e)** the San Juan Mountains.
SNOTEL stations are shown by blue dots. The yellow triangle indicates the U.S. Geological Survey Gage 12082500 on the Nisqually River.

Table 1. Metadata for western United States SNOwpack TELemetry (SNOTEL) stations used to generate the phase diagrams.

Station Name	Elev. m)	Lat ($^\circ$N)	Lon ($^\circ$W)	Start Date	Snow Climate
CSS Lab, CA	2201	39.33	-120.37	Oct 1983	Maritime
Mill-D North, UT	2733	40.66	-111.64	Oct 1988	Intermountain
Mount Rose Ski Area, NV	2683	39.32	-119.89	Oct 1980	Intermountain
Paradise, WA	1564	46.78	-121.75	Oct 1980	Maritime
Red Mountain Pass, CO	3414	37.89	-107.71	Oct 1980	Continental
Tahoe City Cross, CA	2072	39.32	-120.15	Oct 1980	Maritime
Virginia Lakes, CA	2866	38.07	-119.23	Oct 1978	Intermountain

2.2 Gridded Observational Products

65 To add a spatial component to station-based SWE and precipitation phase diagrams, we utilized daily gridded 4 km resolution estimates of SWE for the continental U.S., herein called the University of Arizona SWE reanalysis (UAswe; Zeng et al. (2018); Broxton et al. (2019)). The UAswe product spans WYs 1982–2020. Daily, gridded 4 km spatial resolution precipitation was acquired from gridMET (Abatzoglou, 2013).Phase diagrams can be applied to any long-term daily *in-situ* and/or gridded SWE product and is not limited to the observational products chosen in this study. Examples of watershed-averaged phase diagrams

70 are presented and compared with nearby SNOTEL stations for two, eight digit U.S. Geological Survey Hydrologic Unit Codes (HUC-8) watersheds Seaber et al. (1987) in the Sierra Nevada (The Upper Yuba River Basin and the Tuolumne River Basin).

3 Methods

3.1 Visualizing snow drought with a phase diagram

The concept of phase diagrams were initially developed by Ludwig Boltzmann, Henri Poincaré, and Josiah Willard Gibbs

75 (Nolte, 2010). The intent was to represent all possible states of a dynamical system, such as a particle's position and momentum. Many disciplines now use phase diagrams (also referred to as phase space diagrams)—including nonlinear dynamics, chaos theory, as well as statistical and quantum mechanics. Each parameter of the system in phase diagrams are represented by an axis of a multidimensional space. In a two-dimensional system, each point on the phase plane represents a combination of the system's parameters, with the evolution of the system's state through time tracing a line called the phase space trajectory.

80 The phase space trajectory begins at the point representing the initial conditions. Depending on the application, the trajectory continues indefinitely or until the time period of interest has elapsed.

Inspired by the simplicity of phase diagrams, specifically the Wheeler-Hendon phase diagrams used to track the phase and life cycle of the tropical intraseasonal Madden-Julian Oscillation (Wheeler and Hendon, 2004), our purpose is to show how this visualization approach can track SWE and precipitation conditions during the cool season. We aim to track the phase space of

85 cool season mountain hydroclimate in order to link the trajectory of snow drought conditions (dry and warm; (Harpold et al., 2017)) to the hydrometeorological events (Hatchett and McEvoy, 2018) shaping the trajectories. Thus, phase diagrams can be used to diagnose snow drought onset, termination, duration, type, and severity as well as explore timing and characteristics of 'drought-busting storms'. By implicitly including these mixture effects, phase diagrams provide a unique perspective over time series plots. For instance, phase diagrams can be used to more clearly show the abrupt changes in one or both variables during

90 major accumulation or melt events.

3.1.1 Creating the Snow Drought Phase Diagram

For each station, we calculated daily percentiles of accumulated precipitation and SWE from 1 November to 31 May using a seven-day moving window centered on each calendar day. We calculated percentiles using the period of record. Following Huning and AghaKouchak (2020a), we used the U.S. Drought Monitor "D scale" (Svoboda et al., 2002) to characterize snow

95   drought as abnormally dry (D0), moderate drought (D1), severe drought (D2), extreme drought (D3), and exceptional drought
(D4) for values between the 30th-20th, 20th-10th, 10th-5th, 5th-2nd, and below the 2nd percentiles, respectively. Following
the Drought Monitor scale, snow drought is defined as SWE percentiles less than or equal the 30th percentile, which is slightly
more inclusive than Marshall et al. (2019) who selected the 25th percentile as their threshold. Accumulated precipitation
percentiles were plotted on the x-axis and SWE percentile on the y-axis. Each daily point was coloured by the corresponding
100   month and connected by a line to create the phase trajectory. Snow drought severity, following the D scale, were denoted by
colored lines. We defined the start of snow drought phase diagrams at the beginning of the WY (1 October). Each trajectory
point is binned by a unique color for a given WY month and the first day of each month is indicated by an emboldened letter.
We selected the 31 May for the termination of trajectories, denoted by a gold star. By the end of May, most water-related
decisions based upon snowpack have been made.

3.2   Analysis of Gridded Products

105

For each 4 km SWE grid cell, we calculated daily percentiles of median SWE from 1 October–31 May for WYs 1982–2020,
again using a seven-day moving window. The same approach was performed for gridMET precipitation. Snow drought is
defined similarly as above, when SWE is at or below the 30th percentile. HUC-8 boundaries were used to calculate basin
averages (means) for the gridded products whose grid points fell on or within the HUC-8 boundary.

3.3   Cumulative Discharge Calculations

110

Cumulative discharge at the Nisqually River U.S. Geological Survey stream gage was calculated for all complete WYs starting
on the first day 1 Oct. For each day until the end of the WY (30 Sept), the accumulated discharge was calculated. For each
WY, we calculated the date when 50% of the WY total accumulated discharge occurred. Median dates of 50% of WY total
discharge were calculated using the full period of record.

4   Results and Discussion

115

4.1   An Example Annotated Phase Diagram

WY2020 was characterized by notable snowpack and precipitation variability throughout the cool season in the northern Sierra
Nevada (Figure 2a). Both fall and late winter featured near record-low precipitation and snowpack at the Central Sierra Snow
Laboratory (CSS Lab). The upper right quadrant represents wet and snowy "Big Year" conditions when both accumulated
120   precipitation and SWE exceed the 50th percentile. The upper left indicates SWE was above the median but accumulated
precipitation was below. Trajectories into this "Dry But Snowy" quadrant can result from dry fall conditions followed by
appreciable snowfall, especially in places that normally receive fall precipitation as rain, or in lower elevation, warmer locations
when anomalous snowfall has occurred instead of mixed rain and snow events. A drying fall has been identified as one signal
of climatic change in California (Luković et al., 2021). This drying could induce a systematic leftward shift in future phase

125 diagram trajectories during the 21st century. During the melt season, persistent cold and dry conditions can drive trajectories upwards into the first or second quadrants as snow melts slower than expected historically, as occurred during May 2020.
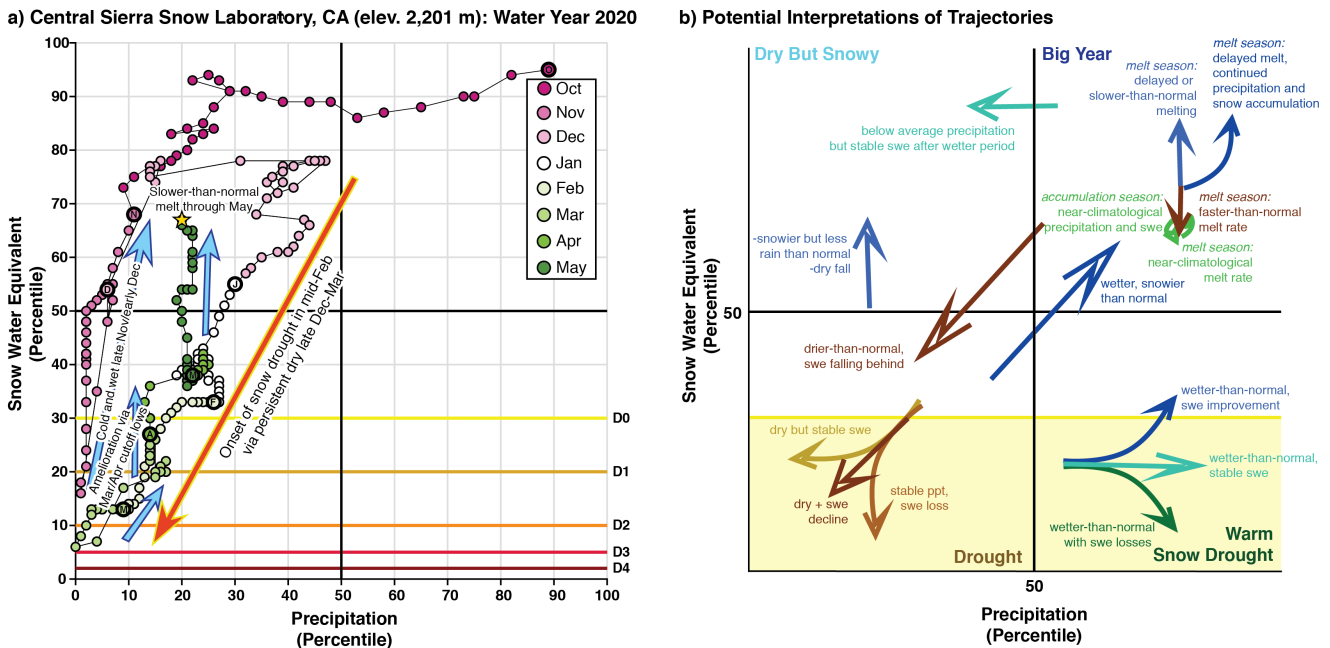
Figure 2. (a) Annotated phase diagram showing 1 October, 2019 to 31 May, 2020 at the Central Sierra Snow Laboratory (CSS Lab), California. Percentiles are calculated based on period of record data. **(b)** Conceptual phase diagram showing potential physical interpretations of seasonal evolution of various trajectories.

Dry snow drought conditions (meteorological drought) are identified in the lower left (third quadrant) when SWE falls into the D0-D4 range (i.e., less or equal to the 30th percentile) and accumulated precipitation is below the median. We defined warm snow drought when satisfies snow drought conditions and accumulated precipitation is greater than the median (lower

130 right, or fourth quadrant). To facilitate connecting various trajectories of phase diagrams with driving processes, the annotated figure is paired with a conceptual diagram showing potential physical interpretations (Figure 2b).

The start of WY2020 was characterized by bottom 3rd percentile precipitation conditions with low (bottom 20th percentile) snowpack at the CSS Lab (Figure 2a). Precipitation falling as snow led to rapid improvement from snow drought into the "Dry But Snowy" quadrant during late November into December, with precipitation recovering to near-normal by mid-December.

135 Persistent dry conditions lasting from late December through mid-March, driven by a blocking ridge west of North America (Gibson et al., 2020), yielded snow drought onset in late January. Above-normal temperatures, dry conditions, and seasonally-induced shifts in solar insolation in late February and early March caused snowpack declines to accelerate, reaching a minimum value in the 5th percentile. Given that California receives the majority of its annual precipitation between December and March, dry spells will quickly lead to declines in precipitation percentile (trajectories move leftward; Figure 2a). WY2020, like other

140   Sierra Nevada drought years, was notable for its lack of atmospheric river (AR) landfalls (Hatchett et al., 2016). ARs produce abrupt upwards and/or rightwards trajectories in the phase diagram via heavy precipitation (Guan et al., 2010) enhanced by orography (Huning et al., 2017). Snow drought amelioration in late March occurred when heavy snowfall resulted from a slow-moving cutoff low pressure system (O'Hara et al., 2009). By 1 April, the historically assumed peak timing of snowpack in the wUS (e.g., Huning and AghaKouchak (2020b)), snow drought conditions remained but had improved from the 5th to nearly

145   the 30th percentile, though precipitation remained in the bottom 15th percentile. Another cutoff low in early April provided additional snow that terminated snow drought conditions, however accumulated precipitation remained below the median. This further highlights the importance of late spring (i.e., post-1 April) meteorological events in improving hydroclimatic conditions and a potential pitfall of assessing drought conditions at a single point in time. The remainder of April and May were drier-than-normal, but snowmelt occurred slower than climatology, with above-median snowpack observed in mid-May. By annotating

150   the phase diagram, the story of the cool season can be expressed to show the key events producing observed outcomes.

4.2   Snow Drought Variation in Time and Space

Weather events drive elevation-dependent changes in snowpack and snow drought conditions (Hatchett and McEvoy, 2018). In regions located near climatological expected rain-snow transition elevations (Jennings et al., 2018), such as the Sierra Nevada, individual storms can produce dramatically different responses in snowpack spatial variability and magnitude. ARs are a

155   common type of storm event yielding variable snowpack and hydrologic responses as a result of heavy precipitation with high snow line elevations (Hatchett et al., 2017; Hatchett, 2018; Henn et al., 2020) or with snow line elevations that vary widely over the duration of the storm (Lundquist et al., 2008; Hatchett et al., 2020).

     WY2018 was emblematic of the aforementioned variation in rain and snow transition elevations as both elevation- and spatially-dependent responses to storms and dry spells occurred in the Sierra Nevada (Figure 3). WY2018 began with varying

160   precipitation and SWE percentiles between three stations, again in the "Dry But Snowy" quadrant at the lower elevation stations (CSS Lab and Tahoe City Cross) and near climatology for the high elevation station (Mount Rose Ski Area). A late November AR event was followed by a multi-month dry spell that terminated in late February. Snowpack and precipitation conditions improved markedly in March, (colloquially termed a "Miracle March"), due to persistent stormy conditions associated with multiple landfalling ARs and/or midlatitude cyclones.

165   To highlight the elevation-induced heterogeneity of snowpack response within WY2018, we investigate three different stations situated along a similar longitude (Figure 1c). The late November warm and wet storm caused the CSS Lab and Tahoe City Cross (Figure 3a-b); both maritime snow climates) to shift rightwards and then downwards into the warm snow drought quadrant because much of the precipitation fell as rain. The CSS Lab is located along the Sierra Nevada crest while Tahoe City Cross is located further east in the rain shadow of the Sierra Nevada crest. Unlike the other two stations, the higher elevation

170   Mount Rose Ski Area (hereafter "Mount Rose"), located further east in the Carson Range in a more intermountain snow climate (colder and drier than a maritime snow climate), received all snow. Mount Rose began the meteorological winter with 80th percentile precipitation and SWE ("Big Year"; Figure 3c). The CSS Lab and Tahoe City Cross received snow early in December, briefly moving each location out of warm snow drought. During the subsequent dry spell, the lower elevation CSS
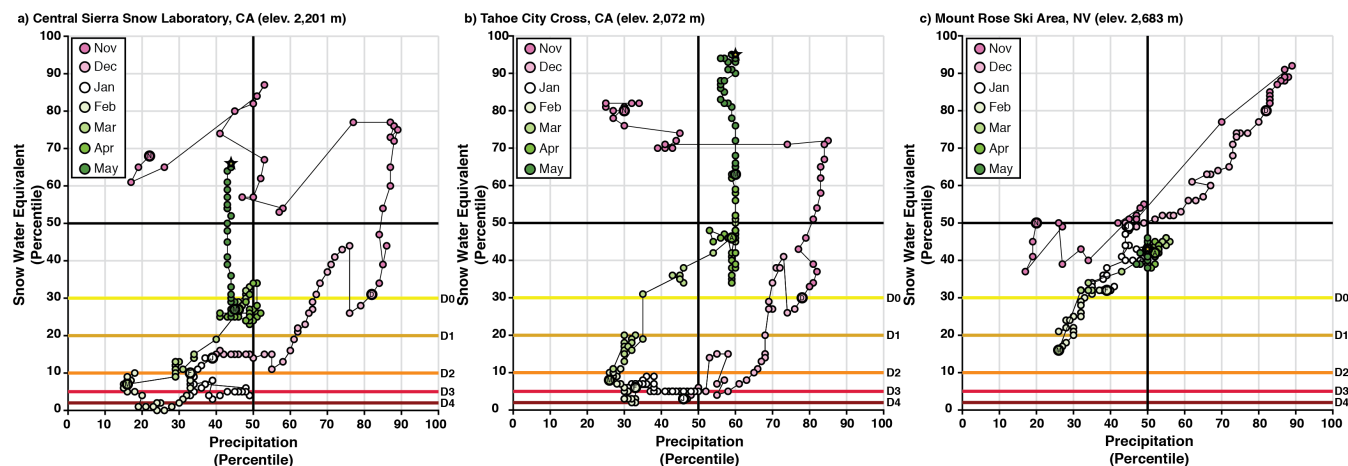
Figure 3. An elevation-longitudinal examination of snow drought conditions during water year (WY) 2018 in the northern Sierra Nevada of California and Nevada. Stations are ordered from west to east: **(a)** CSS Lab, **(b)** Tahoe City Cross, and **(c)** Mount Rose Ski Area.

Lab and Tahoe City Cross stations both moved leftward from warm snow drought into dry snow drought, with a 30 percentile

175 point decline in SWE through December. Dry snow drought conditions began at Mount Rose in early February. Importantly, the role of elevation is highlighted ($\sim$600 meter range between stations) with the colder Mount Rose experiencing less dramatic snowpack declines (reaching a minimum of the 16th percentile) compared to the warmer CSS Lab (minimum of 1st percentile) and Tahoe City Cross (minimum of 2nd percentile).

The return of North Pacific storminess during late February into March brought notable improvement in precipitation and

180 snowpack conditions. This period also highlighted how snow drought amelioration is influenced by snow climate type and elevation. During this period, Mount Rose received all precipitation as snow. As a result, SWE improved by 30 percentile points (out of snow drought) while precipitation improved from the 26th percentile to 52nd percentile (Figure 3c). The maritime CSS Lab improved SWE by 35 percentile points from the lowest on record for the date in late February to non-snow drought conditions by late March. Precipitation also improved by approximately 35 percentile points, back to near median values. The

185 cold March storms demonstrated a weaker rain shadow and generally lower snow levels. This improved SWE at the Tahoe City Cross from the 2nd percentile to above the 40th percentile while precipitation also improved from the 26th to the 60th percentile between late February and early April (Figure 3b). As a result of "Miracle March", 1 April SWE conditions were closer to median than reflected by the majority of the winter, similar to WY2020 (Figure 2a). The record to near-record low, late winter SWE at the lower elevation CSS Lab and Tahoe City Cross are thus hidden by a single point-in-time perspective.

190 WY2018 and WY2020 demonstrate the importance of a complete WY perspective regarding the assessment of evolving snow drought conditions, namely the importance of a few large precipitation events.

4.3 Warm Versus Dry Snow Drought: Implications for Runoff Timing

The warming-induced shift in precipitation phase from snow to rain has been shown in historical trends in the wUS (Lynn et al., 2020) and is projected to continue in a warmer world (Klos et al., 2014; Rhoades et al., 2018c; Musselman et al.,
195 2018). Precipitation phase transition from snow to rain will result in more frequent warm snow droughts (Marshall et al., 2019; Huning and AghaKouchak, 2020a). This increase will disproportionately impact climatologically warmer maritime snow climates (Dierauer et al., 2019) with important implications on the headwater hydrology and downstream reservoir management strategies of these watersheds (Huang et al., 2018; Rhoades et al., 2018a; Yan et al., 2018; Rhoades et al., 2018b; Ullrich et al., 2018). To provide a comparison of WYs that experience comparable snow drought conditions, but differing
200 drivers, we compared the WY2001 dry snow drought (Figure 4a) to the WY2015 warm snow drought (Figure 4b) at Paradise, Washington in the Pacific Northwest on the south flank of Ti'Swaq' (Mount Rainier; Figure 1b). The WY2015 warm snow drought in the Pacific Northwest was a motivating and formative WY for the development of modern snow drought research (Cooper et al., 2016).

Paradise spent the majority of the cool season of WY2001 in the bottom 10th precipitation percentile, a substantial difference
205 from WY2015 when precipitation was between the 60th and 88th percentile between December and April. The warm snow drought resulted from an anomalous amount of precipitation largely falling as rain in the early portion of winter. Snowpack conditions marginally improved throughout WY2001 from below the 10th percentile in February to the 20th percentile by the end of the cool season (Figure 1a). However in WY2015, Paradise maintained fairly consistent SWE percentiles below the 10th percentile from February to May. The leftward trajectory of precipitation during February 2015 is indicative of drier-
210 than-normal conditions followed by generally dry conditions (Figure 1b). Weak snow drought amelioration occurred in 2001, minimizing its water resource impacts, whereas none occurred in 2015, further highlighting the importance of monitoring snow drought conditions, and type, over an entire WY.

Figure 4(a-b) shows the entire WY phase diagrams and a SWE spatial extent snapshot at various times (d-k), relative to median climatology, for WY2001 and WY2015. We also highlight the differences in hydrologic outcomes between these dry
215 and warm snow drought years (Figure 4c). WY2001 had the second lowest cumulative flows for the Nisqually River in the period studied (WY1943–2019), but 50% of the cumulative WY2001 flow occurred 30 days *later* than the median date (3 April) at which half the Nisqually flow occurs. In contrast, WY2015 demonstrated middle-of-the-range total WY flow (48th of 77 years) but achieved 50% of the WY flow 56 days *earlier* than average. This indicates a key difference between the WYs. WY2015 had less snow water stored later into the season, which markedly influenced streamflow. During both seasons, despite
220 the vastly different precipitation regimes, spatial SWE anomalies are not markedly different during mid-December (Figures 4d and 4h), mid-January (Figures 4e and 4i), or late February (Figures 4f and 4j). Consistent with lower SWE percentiles at Paradise during WY2015 compared to WY2001, as shown on the phase diagrams, SWE anomalies are modestly more negative. The lack of mountain snowpack during WY2015 was more notable than WY2001 (Figures 3g and 4k). The comparatively better spring snowpack in WY2001 likely helped maintain flows later into the year despite an otherwise dry year.
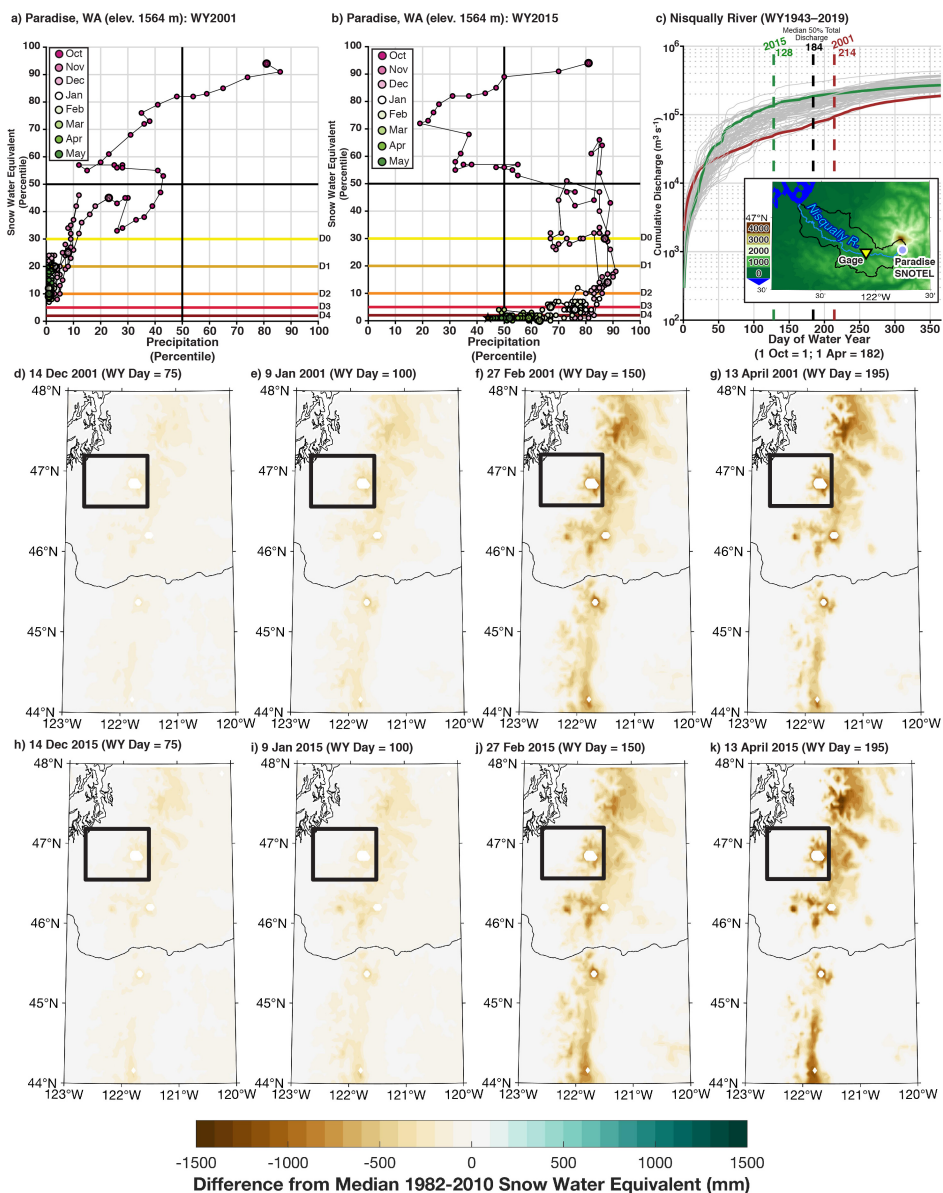
Figure 4. Comparison of dry **(a)** and warm **(b)** snow drought conditions in the Pacific Northwest at Paradise, Washington during water years (WY) 2001 and 2015, respectively. **(c)** Cumulative discharge (in $\mathrm{m^3 s^{-1}}$) from the Nisqually River with vertical dashed lines indicating the date at which 50% of the total WY runoff occurred. **(d–g)** Spatial snow water equivalent anomalies (in mm) during WY2001 from the UAswe product (Zeng et al., 2018). **(h–k)** As in **(d–g)** but for WY2015.

4.4 Interannual Variability

Enhanced interannual hydroclimate variability is expectation of a warming climate (Boer, 2009; Pendergrass et al., 2017) with comparisons of extreme years and their outcomes providing valuable object lessons for water managers and other resource planners (Hossain et al., 2015; Sterle et al., 2019). Phase diagrams allow for direct comparisons between WYs, helping to identify key differences in hydroclimate variability for a particular region of interest. As a proof of concept, Red Mountain Pass, located in a high elevation, continental snow climate within the San Juan Mountains of southwestern Colorado, is used to compare two late cool season outcomes that represent two hydroclimatic extremes. The majority of WY2011 showed phase trajectories in the 'Big Year' first quadrant (Figure 5a) after a slightly below-average start to snowpack totals between October and early December. An active December increased SWE and precipitation percentiles. Active weather continued in April and May, preventing snowmelt and causing precipitation and SWE percentiles to increase. WY2012 began with above-average precipitation and snowpack in fall but drier-than-normal conditions throughout winter which resulted in dry snow drought onset in December (Figure 5b). Modest snow drought amelioration occurred in early March, but with a few exceptions in April, dry conditions persisted through May. This led to the onset of dry snow drought, again, via rapid snowmelt and below-average precipitation.

Spatial SWE distributions are consistent with the phase diagrams (Figure 5c-j). In both years, SWE anomalies increased throughout the accumulation season and then accelerated in late spring. Compared to the emerging drought signal during WY2012, WY2011 did not demonstrate widespread positive SWE anomalies throughout the year. Between January and April, lower elevation regions experienced below-normal SWE anomalies (Figure 5c-d), whereas higher elevations had above-normal SWE. This difference resulted from above-normal temperatures and below-normal precipitation, likely driven by snow-albedo feedbacks that were enhanced at lower elevations where snowmelt occurred (Groisman et al., 1994; Stieglitz et al., 2003).

4.5 Basin-Averaged Snow Drought Phase Diagrams

Aggregating spatially distributed information to the HUC-8 scale allows the creation of phase diagrams where few or no *in situ* observations exist. If such observations do exist, watershed-aggregated phase diagrams can be compared against station data, as shown in Figure 6 for WY2020 (see Section 4.1). We examine two Sierra Nevada watersheds, the relatively low elevation Upper Yuba River Basin and the relatively high elevation Tuolumne River Basin. Both have nearby SNOTEL stations, the CSS Lab station sits at the headwaters of the Yuba River while the Virginia Lakes station is located on the lee of the Sierra Nevada crest northeast of the Tuolumne River Basin.

In both cases, similarities exist between the SNOTEL and watershed-aggregated phase diagrams (Figure 6). The SNOTEL stations, which are located at higher elevations in the watershed, show wetter (above median) and snowier (above median) early season conditions during October and November (Figure 6a,c) whereas the watersheds show below median SWE and precipitation (Figure 6b,d). Late November and December brought substantial SWE improvement, with the Upper Yuba Basin moving into the "Dry But Snowy" quadrant (Figure 6b) and the Tuolumne River Basin extending further rightwards into the "Big Year" quadrant (Figure 6d). Virginia Lakes also improved into the "Dry But Snowy" quadrant (Figure 6c). Both
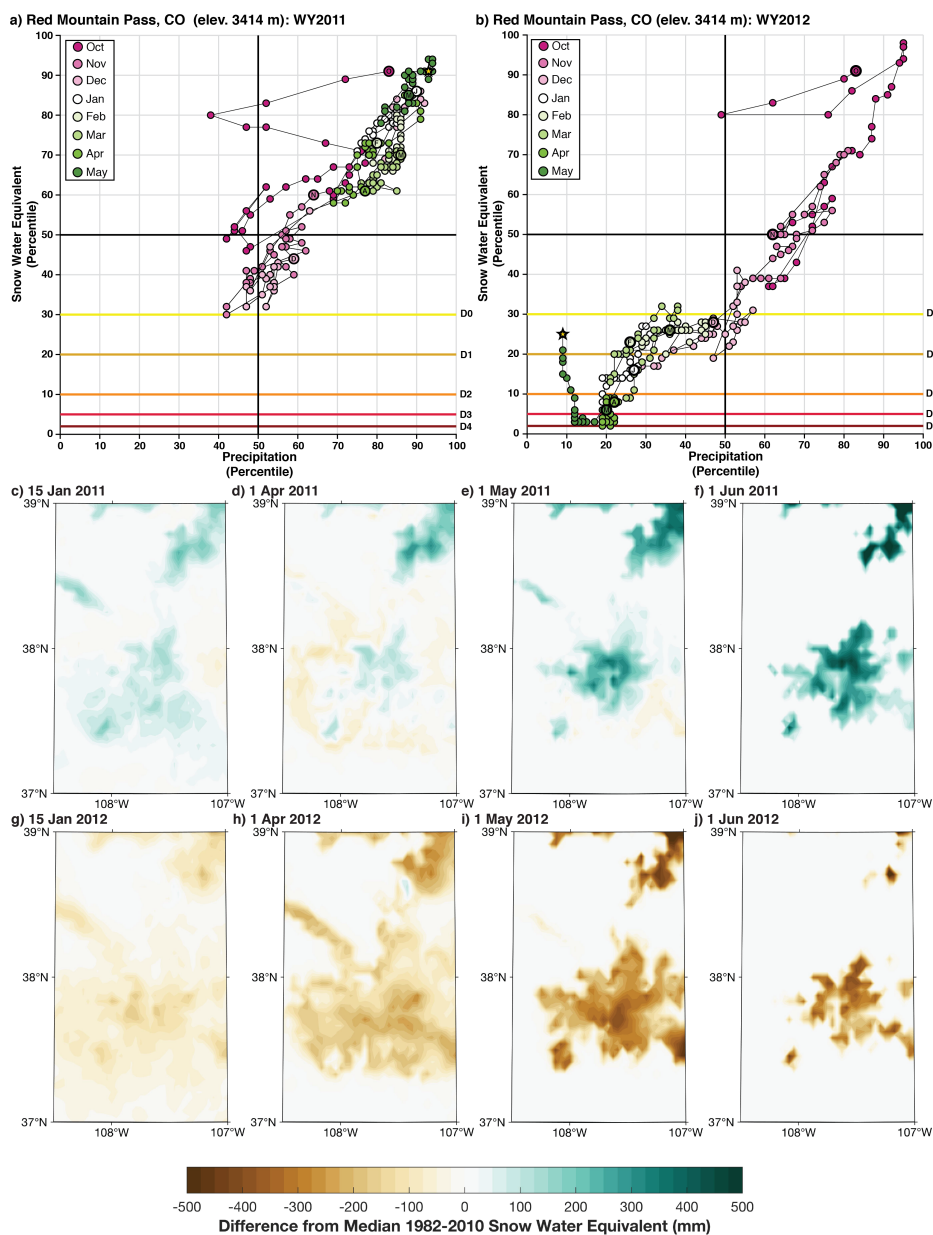
Figure 5. Comparison of an anomalously snowy and wet "big year" **(a)** and anomalously dry year **(b)** in the San Juan Mountains at Red Mountain, Colorado during water years (WY) 2011 and 2012, respectively. **(c-f)** Spatial snow water equivalent anomalies (in mm) during WY2011 for midwinter, early, middle, and late spring from the UAswe product (Zeng et al., 2018). **(g-j)** As in **(c-f)** but for WY2012.

regions followed similar trajectories downwards and to the left (SWE and precipitation falling behind; (Figure 2b)) during the
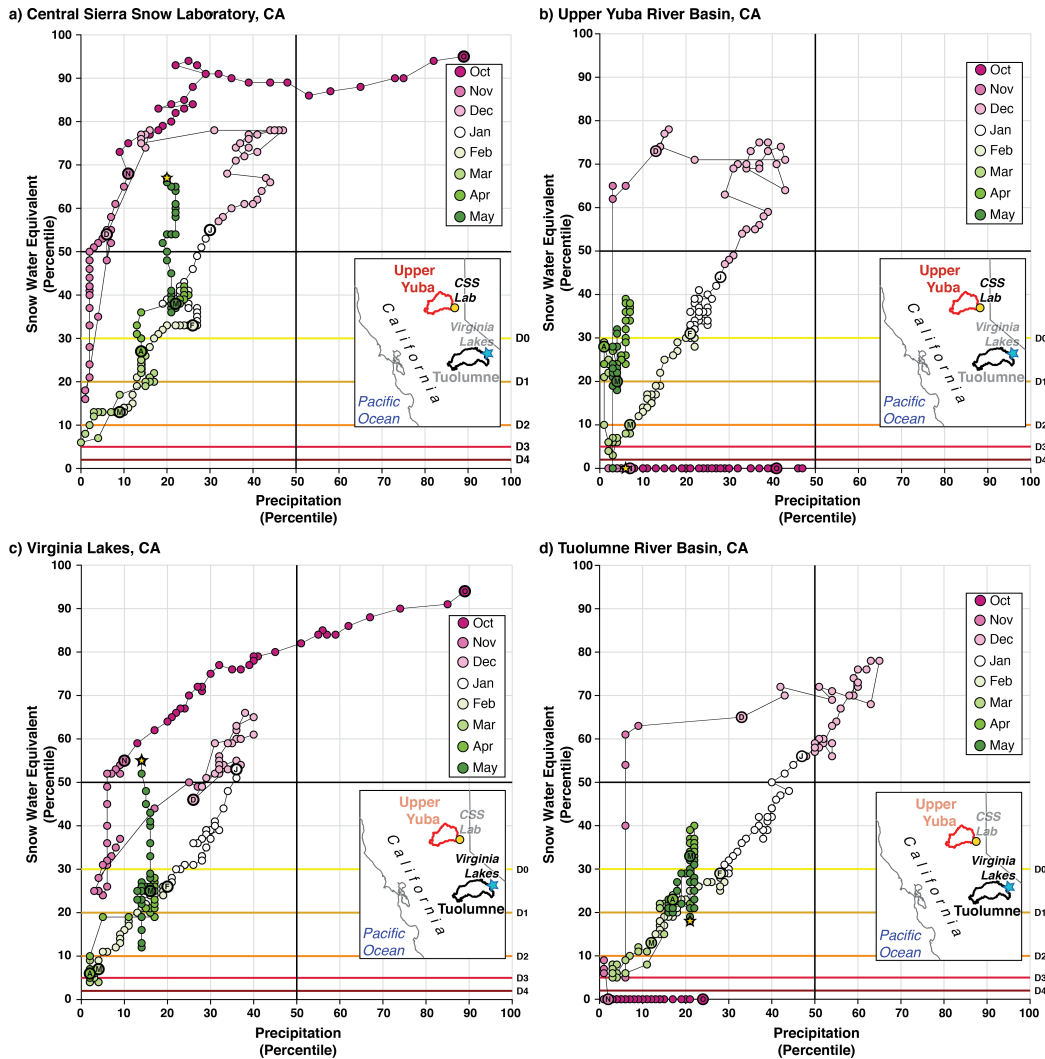
Figure 6. Phase diagrams for water year 2020: **(a)** CSS Lab SNOTEL, **(b)** Upper Yuba River Basin HUC-8, **(c)** Virginia Lakes SNOTEL, and **(d)** Tuolumne River Basin HUC-8. Locations of watersheds and SNOTEL stations are noted on inset maps.

extremely dry period spanning late December into mid-March and then underwent modest SWE recoveries with the active

260   spring ("Miracle March").

By the end of the cool season (31 May), the higher elevation Tuolumne River Basin experienced wetter conditions (22nd percentile) compared to the Upper Yuba Basin (5th percentile precipitation) as well as exiting D0 snow drought (SWE > 30th percentile precipitation) while the Upper Yuba Basin remained in D2 (22th percentile SWE). This may reflect orographically enhanced precipitation and/or higher snowline elevation during the spring storms. The SNOTEL stations, likely by virtue

265   of their location at higher elevation, demonstrated opposite melt-out signals to the basin-aggregated phase diagrams. The

SNOTELs increased in SWE percentile through May while the basin-wide percentiles declined. This result may stem from the inclusion of lower elevation terrain in the basin aggregations whose snow rapidly melts out during drought years (potentially accelerated by snow-albedo feedbacks, e.g., Groisman et al. (1994)). Despite these differences, the basin-aggregated phase diagrams appear reasonably representative in capturing the broader hydroclimate conditions interpreted from phase trajectories.

4.6 Towards Visualizing the Type and Extent of Snow Drought Across Space

We applied SNOTEL station data to create the phase diagrams, but a challenge in mountain environments is the lack of reliable, well-distributed, long-term observations. In lieu of station data, gridded observational products commonly inform natural resource decision-making and research efforts. The necessary components exist to create phase diagrams using gridded meteorological products (Daly et al., 2008; Abatzoglou, 2013), observation-based snow datasets (Zeng et al., 2018; Margulis et al., 2016), and output from hydrological simulations (Livneh et al., 2015). The challenge is how to aggregate spatial information to become meaningful in complex terrain. We have performed a first step towards this goal. Initial methods to broaden the approach could be performed by: (1) binning regions by similar elevation, watershed, slope, aspect, and/or land cover type; (2) identifying areas that co-vary together in time and space using techniques such as principal component or cluster analysis; and (3) subjective grouping based on anecdotal information from managers. Creating meaningful phase diagrams using spatially distributed information is the primary goal of our ongoing research. This will allow evaluation of snow drought in regions without long-term snow-observing networks such as in the northeastern U.S. or other high mountain areas worldwide. Towards this end, we next provide examples of how spatially distributed products can visualize snow drought.

4.6.1 Snapshots from Water Year 2015

Using WY2015 as an example, gridded SWE and precipitation allow visualizing the spatial extent and type of snow drought. Peak warm snow drought conditions in the Pacific Northwest were occurring in January (Figure 7a), consistent with the Paradise SNOTEL phase diagram (Figure 4b). In January, much of the Intermountain West and Rocky Mountain regions had near-average or above average (percentiles greater than the 50th, represented in purple), while several ranges in the southern tier of the wUS (e.g., California's Sierra Nevada, the southern Basin and Range, and the Uinta Mountains in Utah) were experiencing dry snow drought conditions. By the 1 February (Figure 7b) an expansion of areas experiencing dry snow drought occurred throughout the central and southern Rocky Mountains. Warm snow drought had started to transition to dry snow drought in the Pacific Northwest. Dry conditions continued through February (Figure 7c). By 1 April, nearly all mountain regions were experiencing snow drought conditions (Figure 7d). Exceptions include the far northern Rockies, a few small areas in the Colorado Rockies, and the far northern Cascades.

The transition to dry snow drought in the Pacific Northwest (Figure 7d) was also observed at the Paradise SNOTEL (Figure 4b). While the hydrologic outcome of the early winter warm snow drought included earlier runoff timing resulting from more frequent mid-winter runoff following rain-on-snow and rain instead of snow ((Hatchett and McEvoy, 2018); Figure 4c), the 1 April conditions indicate dry snow drought both spatially (Figure 7d) and at the station level (Figure 4b). This demonstrates the value of tracking snow drought and precipitation through time, as following the temporal evolution of hydroclimate allows
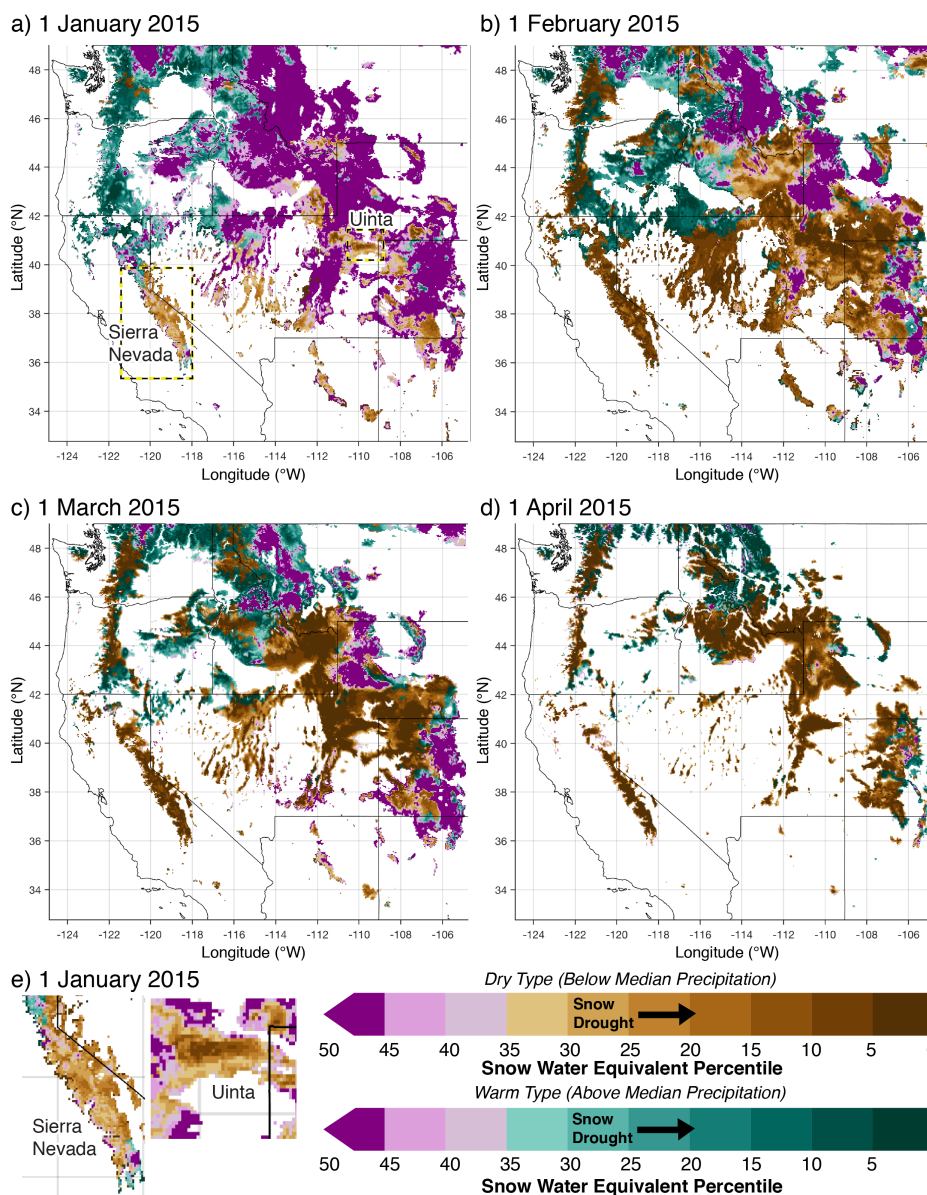
Figure 7. Spatial extent of snow drought conditions across the western United States on: **(a)** 1 January 2015, **(b)** 1 February 2015, **(c)** 1 March 2015, and **(d)** 1 April 2015. **(e)** The differing snow drought patterns across elevation in the Sierra Nevada (percentiles increase with increasing elevation) and the Uinta Mountains (percentiles decrease with increasing elevation). For clarity, only grid cells observing seasonal snowpacks (Hatchett, 2021) are shown.

outcomes (e.g., runoff and spatial patterns of snowpack anomalies) to be explained with more nuance. Such explanation is
300   important as similar end-of-season SWE anomalies in space (compare Figures 4g, 4k, and 7d) demonstrate markedly different

hydrologic outcomes (Figure 4c). Last, Figure 7e highlights an example of the differing elevational response of snow drought in the Sierra Nevada (percentiles increase with increasing elevation) and the Uinta Mountains (percentiles decrease with increasing elevation) for the same midwinter time. This example shows how sub-seasonal snowpack heterogeneity could create differing melt-season responses (i.e., earlier snow loss at lower elevations with increasing radiation and springtime warming) or ongoing avalanche hazards (i.e., higher elevation snowpacks are more prone to weakening when shallow).

4.6.2 Tracking Interannual Snow Drought Magnitude and Extent

The varying categories of snow drought and their spatial extent over large swaths of the wUS can be tracked through time (Figure 8). Sub-selecting snowpacks typically classified as seasonal in the wUS (Hatchett, 2021) using a median value of the snow seasonality metric (Petersky and Harpold, 2018) exceeding 0.5, three important time periods are examined. The first two times, 24 December (Figure 8a) and 1 March, represents two important holiday periods when snow recreation-based tourism has an outsized impact on mountain economies (Hagenstad et al., 2018). The third time, 1 April (Figure 8c), as well as 1 March (Figure 8b), represent important decision-making times for wUS water resources Lynn et al. (2020).

In all cases, interannual variability ranges from less than 10% to more than 60% in December (Figure 8a) and March (Figure 8b). The maximum amount of area in snow drought on 1 April is less than 50%. The WY2015 snow drought stands out (Figure 8b-c; see also Figure 6c-d), especially given the amount of area in the more severe snow drought categories (D2-D4). December and March snow droughts in the early 1990s appear to have undergone amelioration during March, as indicated by decreasing area.

Applying a Mann-Kendall test for trend (Hamed and Rao, 1998) suggests 1 April and 24 December have experienced long-term increases in the amount of seasonal snowpacks in snow drought. The 1 April trend of 2.3% decade^{-1} is more significant (p=0.00037) than the 3.3% decade^{-1} trend for 24 December (p=0.06). The trend of 0.3 % decade^{-1} for 1 March was not significant (p=0.87). These examples could be further extended to the mountain range or watershed scale of interest as well as subset by elevation. They could be extended to show percent of area in snow drought at the daily timescale to track conditions through a given year. In addition, these plots could be decomposed to show percent of area in warm or dry snow drought in order to track physical drivers of snow drought conditions.
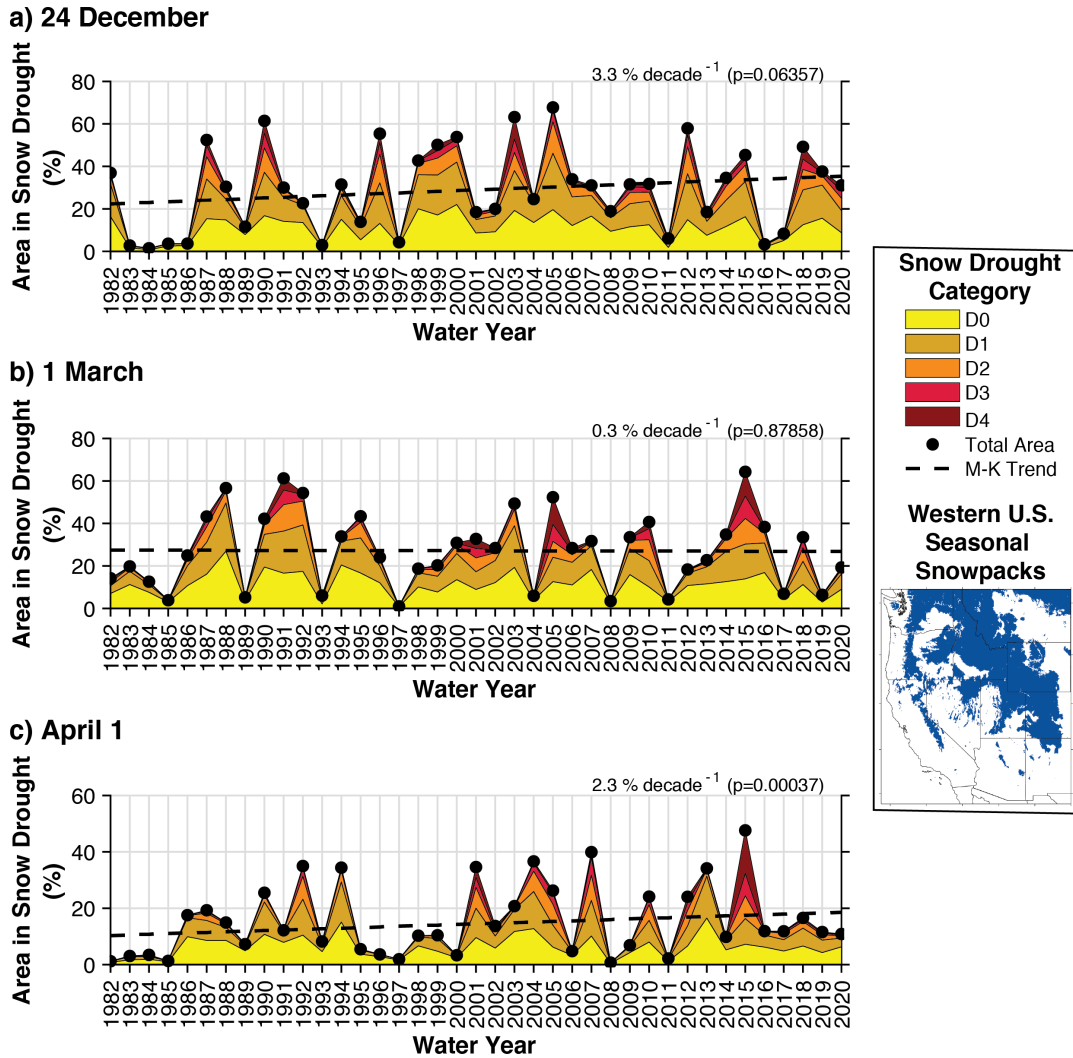
Figure 8. Time series of the percent of western United States seasonal snowpack area in various categories of snow drought (D0-D4) for: 24 December **(a)**, 1 March **(b)**, and 1 April **(c)**. The inset map at right shows the area (in blue) satisfying seasonal snowpacks over which the area calculation is performed.

4.7 Web-based Snow Drought Tracker Description

A snow drought tracker web application has been developed to provide users access to snow drought phase diagrams. The beta version is available at: https://wrcc.dri.edu/my/climate/snow-drought-tracker and simply requires users to set up a username/password to access it. The web tool is updated in near real-time across the wUS and Alaska. The SNOTEL network (Serreze et al., 1999) is the backbone of the tool with over 700 stations providing daily SWE, snow depth, precipitation, and temperature data. An interactive map (Figure 9a-b) allows for station selection via a graphical user interface. Once a station is selected, current year observations are displayed on the "Dashboard" by default (Figure 9c-d). As an example, the Mill-D North station in the Wasatch Mountains of northern Utah is shown (Figure 1b). The "Dashboard" will also display the most recent daily updated snow drought phase diagram (starting on October 1st of the WY2021; Figure 9e. The "Almanac" has several tabs showing daily SWE, snow depth, and precipitation absolute values, and percent of average SWE (Figure 9c). Note that because percent of average is more commonly used by managers, the first iteration of the tool uses percent of average (and the 80% threshold used by Hatchett and McEvoy (2018)) instead of percentiles and Drought Monitor thresholds as otherwise focused on in this manuscript. From the "Almanac" the month-to-date, calendar year-to-date, and WY-to-date precipitation values and percent of normal can be viewed (Figure 9d). In addition to the current year data found on the dashboard, historical data and graphics can be generated. Phase diagrams can be created for any year in the station record and daily time series plots can be generated for SWE, snow depth, precipitation, and temperature (e.g., Figure 9e). Figures are available to download as PNG or SVG files and historical data can be downloaded in CSV format. Beta testing of the snow drought tracker is being conducted by stakeholders including the National Weather Service, California Department of Water Resources, and state climatologists around the wUS. Other agencies will be encouraged to test the tool after the first round of testing and updates have concluded. Feedback from the testing will be incorporated into future upgrades of the snow drought tracker, with the goal of further developing a web-based product that facilitates and provides a science-to-service-to-practice interface (Jacobs and Street, 2020). Some known limitations and gaps in the current version of the tool include the lack of spatial snow drought information (i.e., river basin composites (Figure 6) or gridded data estimates (Figure 7)) and the need to incorporate elevation gradients into snow drought monitoring.
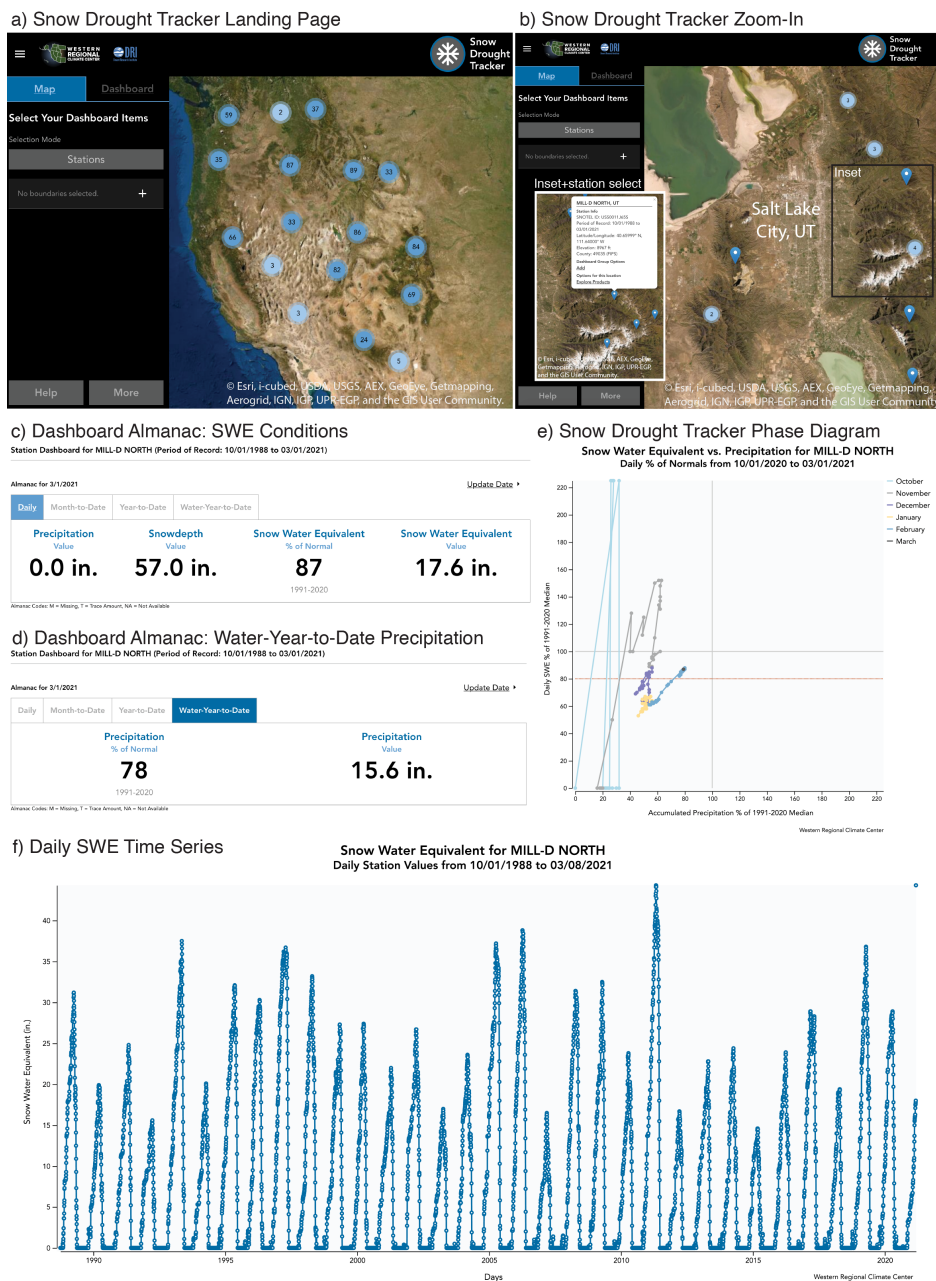
Figure 9. Screenshots from the beta Western Regional Climate Center (WRCC)'s Snow Drought Tracker. **(a)** Dashboard landing page. **(b)** Example screenshot assessing a station in a region of interest (inset). **(c)** Daily information tab from the Almanac. **(d)** Water-Year-to-Date Almanac tab. **(e)** Real-time phase diagram for water year 2021. **(f)** Daily snow water equivalent (SWE) time series for the period of record. Basemaps in **(a)** and **(b)** utilize ArcGIS® Online World Imagery by Esri. ArcGIS® is the intellectual property of Esri and are used herein under license. Copyright ©Esri. All rights reserved. For more information about Esri® software, please visit www.esri.com.

4.8 Limitations

4.8.1 Phase Diagrams

Our snow drought phase diagram visualization approach is not without limitations. By failing to include additional environmental controls on snowpack, such as temperature, radiation, and relative humidity, phase diagrams cannot tell a complete story of the drivers of snow accumulation, ablation, and/or melt. For example, the signal of a rain-on-snow event (McCabe et al., 2007) was captured in the snow drought phase diagrams for Tahoe City Cross (see Figure 3) for an anomalously warm April AR (Hatchett, 2018). This event increased precipitation percentiles though SWE percentiles remained constant. However, when a rain-on-snow event increases net SWE, the phase diagram will not explicitly differentiate this from a snow accumulation event. Dry periods have differing snowpack outcomes during both the accumulation and ablation season depending on temperature (Hatchett and McEvoy, 2018; Xu et al., 2019) as well as how the snowpack energy budget is influenced by the deposition of dust or other light-absorbing particles on snow (Skiles and Painter, 2016; Skiles et al., 2018), cloud cover (Sumargo and Cayan, 2018), and moisture (Harpold and Brooks, 2018). How best to include these additional parameters that help to describes changes in the phase diagram trajectories is an area of future research. Collaborations with natural resource managers, practitioners, and decision makers will be instrumental in the development of locally- or regionally-specific snow drought thresholds. Ideally, such collaborations will facilitate the use of phase diagrams for monitoring efforts (at sub-seasonal-to-inter-annual scales) and be used to evaluate past hydroclimatic extremes to improve real-time water supply monitoring (Sterle et al., 2019).

4.8.2 Percentiles Versus Percent of Median: The Wilson Glade, UT avalanche incident

At present, phase diagrams on the WRCC Snow Drought Tracker show percent of median, rather than percentiles. Percent of median is more commonly used in snow drought communication by the National Integrated Drought Information System's Snow Drought Tracker website (https://www.drought.gov/topics/snow-drought). A difficulty with using a percent of average rather than a percentile-based approach is it does not reflect the distribution of conditions. Percentile-based approaches provide more direct information about a given date's conditions with respect to the range of previously experienced conditions. To highlight the value of a percentile-based approach and how phase diagrams can be employed to assess the evolution of snowpack stability, an example from a 2021 avalanche incident in the Wasatch Mountains is explored.

On 11 February 2021, a skier triggered failure of a deep persistent slab R4-D2.5 avalanche event (R4 implies a large runout relative to path size, D2.5 indicates sufficiently large to bury, injure, or kill a person; Birkeland and Green (2011)) occurred on a northeast aspect at approximately 2900 m in the Wilson Glade region of the central Wasatch Mountains. Despite heroic rescue efforts, four fatalities resulted. A detailed report is available from the Utah Avalanche Center (UAC): https://utahavalanchecenter.org/avalanche/59084. The UAC's avalanche advisory for 11 February was high, indicating large human-triggered avalanches are very likely.

The phase diagram for the Mill-D North SNOTEL (Figure 10a; 3.3 km southeast of the accident site) shows early season November snowfall was followed by prolonged dry conditions into the winter months (downward and leftward trajectory), with
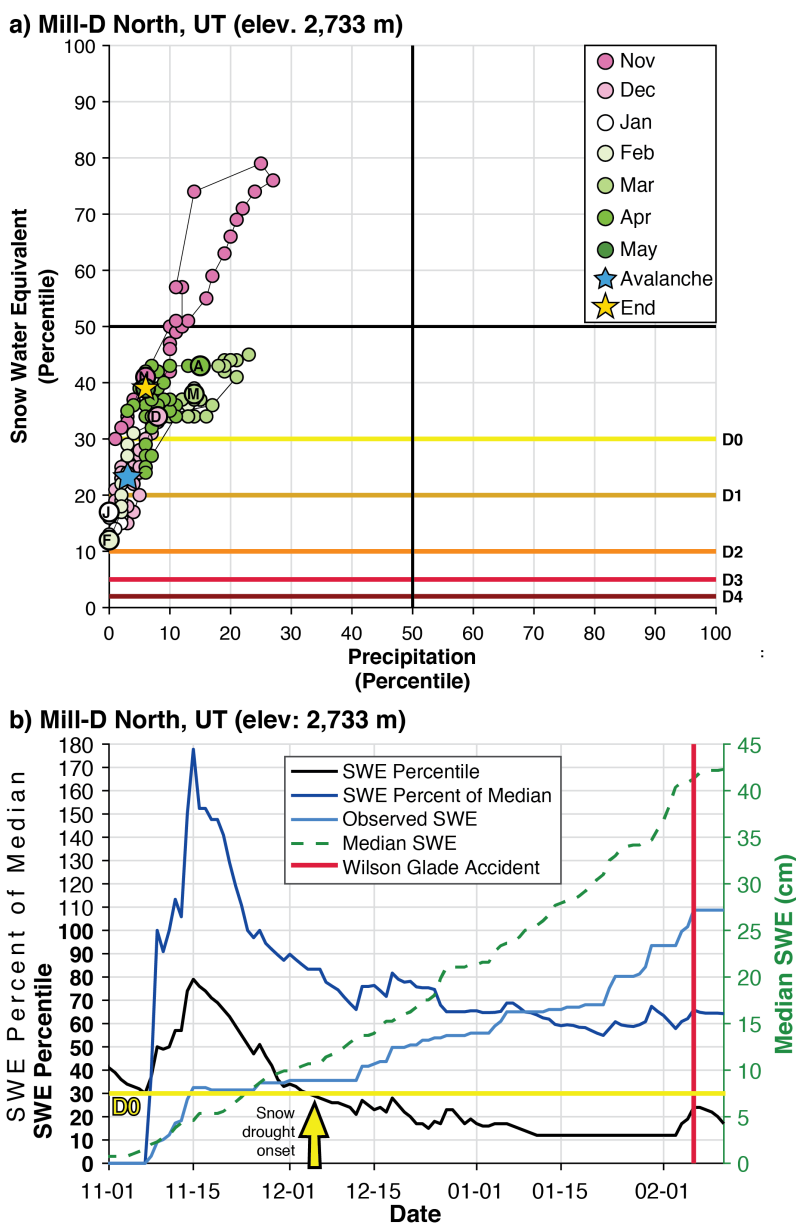
Figure 10. (a) Phase diagram for Mill-D North SNOTEL in the Wasatch Mountains of Utah for WY2021. **(b).** Time series of snow water equivalent (SWE) percentile (bold; left y-axis) and percent of median (left y-axis) and observed and median SWE (cm; dark blue and dashed green lines, respectively; right y-axis). The vertical red line shows the date of the Wilson Glade Avalanche accident. The horizontal gold line shows the percentile associated with "Abnormally Dry" (D0) snow drought conditions.

D0 snow drought onset in early December (Figure 10a and (yellow arrow in Figure 10b)). Note snow drought onset occurs, perhaps non-intuitively, at approximately 85% of median snowpack. This indicates limited variability in SWE at this time and station: large deviations from the median value are relatively infrequent. The late November and early December dry spells led

385 to snowpack accumulation falling behind the climatological average (Figure 10b). While some accumulation occurred during mid-December into early January, the rate of accumulation was less than climatology (Figure 10b), leading to a continued decline into D1 snow drought (Figure 10a). Percent of median SWE hovered around 65% leading up to the avalanche (Figure 10b), though SWE percentiles fell into the D2 category. A transition to more active weather in late January into February followed with gains in SWE that mirrored climatology with little change in SWE percentile or percent of median (Figure 10b).

390 The presence of a shallow snowpack during the dry, low radiation periods in November and December promoted the formation of a persistent weak layer with striated, 3-6 mm faceted grains buried 90 cm deep in the snowpack. According to the UAC, this is the layer where failure occurred on 11 February.

The snowpack conditions leading up to the Wilson Glade avalanche show the potential disconnect between percent of median and percentile. Prior to the loading events, the percent of median values (65%) between December and early February do not

395 directly convey the infrequency of these values as percentiles can. Percentiles show that such conditions occurred only 10-20% of the time. The user's familiarity with a location will govern the meaningfulness of percent of medians through prior experience. On the other hand, percentiles provide perspective for less-familiar users to understand the distribution and state of the snowpack. Percentiles also allow comparisons between locations in terms of snow drought severity. By recognizing both as valuable, the option to view either on the snow drought tracker webtool is a planned improvement. Last, we recommend

400 incorporation of percentiles into accident write-ups, such as provided by the UAC, to give this additional statistical perspective.

5   Conclusions

Our primary goal was to demonstrate a visualization approach to show the temporal evolution of snow drought conditions, and more broadly mountain hydroclimatic conditions, through the cool season. When annotated, phase diagrams help "tell the story" of a snow season and can help communicate the weather and climate events that shaped the outcome of peak snowpack

405 and lifecycle of the snowpack. We provided examples showing a range of applications in various snow climates for extreme years and how additional data such as spatially distributed SWE and precipitation as well as river discharge can further enhance the utility of information provided by phase diagrams. The spatial snow drought maps and basin-aggregated phase diagrams generated using gridded data products demonstrate an approach evaluating snow drought patterns across the landscape or in sparsely observed regions.

410 Our approach can be extended beyond addressing the noted limitations. While our primary purpose was to show the evolution of conditions in the current year, phase diagrams are easily produced for all previous years to allow comparisons of trajectories at seasonal or monthly timescales. These diagrams can incorporate forecasts of precipitation and SWE to show how snow drought conditions may evolve at subseasonal-to-seasonal timescales. For example, inclusion of bias corrected ensembles of medium range to subseasonal forecasts of precipitation and SWE from various forecasting center model(s) can create

415 an ensemble of plausible trajectories (or cone of uncertainty) that would provide a probabilistic perspective to explore snow-drought evolution. They can also be applied to investigate how climate change may permanently alter phase diagram trajectories and/or residence times of WY snowpack conditions in particular quadrants of the phase diagram.

Ultimately, phase diagrams could become useful tools to provide climate services to both the public and decision-making audiences through early warning information on drought type, location, extent, and severity. The goal of these diagrams and

420 the web-based tool is to alleviate some management concerns outlined in Hossain et al. (2015) and Sterle et al. (2019), namely through illuminating water supply uncertainties and enhancing the flexibility of subseasonal-to-seasonal water management practices. By providing another means to communicate climate information, phase diagrams may help further develop the capacity to identify and to rapidly evaluate underlying vulnerabilities within and between human and natural systems that are susceptible to cascading and compounding effects (Jacobs and Street, 2020; Siirila-Woodburn et al., 2021). The Web-based tool

425 producing the snow drought phase diagrams (https://wrcc-staging.dri.edu/my/climate/snow-drought-tracker) presented herein is concurrently being shared with groups responsible for communicating snowpack and mountain hydroclimate information to the public such as the National Weather Service as well as other water and natural resource managers. Our aim is for this information to aid mountain hydroclimate monitoring and drought early warning efforts.

Code availability. All MATLAB code is available upon reasonable request.

430 *Author contributions.* **Benjamin J. Hatchett**: Conceptualization, Investigation, Visualization, Software, Formal Analysis, Writing – Original Draft, Writing – Review and Editing, Funding Acquisition. **Alan M. Rhoades**: Conceptualization, Investigation, Visualization, Formal Analysis, and Writing - Review and Editing. **Daniel J. McEvoy**: Conceptualization, Investigation, Funding Acquisition, Writing – Review and Editing.

Competing interests. The authors declare no competing interests.

435 *Acknowledgements.* We appreciate feedback from Michael Anderson, Sasha Gershunov, Tim Bardsley, and Zach Tolby. Roger Kreidberg provided technical editing and writing advice. Authors Hatchett and McEvoy was supported by the Desert Research Institute Foundation under an Institutional Research Project (IRP) grant and the National Weather Service. Author Rhoades was funded by the Office of Biological and Environmental Research of the U.S. Department of Energy within the Regional and Global Climate Modeling Program program under the "the Calibrated and Systematic Characterization, Attribution and Detection of Extremes (CASCADE)" Science Focus Area (award no. DE-

440 AC02-05CH11231) and the "A Framework for Improving Analysis and Modeling of Earth System and Intersectoral Dynamics at Regional Scales" project (award no. DE-SC0016605).

References

Abatzoglou, J. T.: Development of gridded surface meteorological data for ecological applications and modelling, International Journal of Climatology, 33, 121–131, https://doi.org/https://doi.org/10.1002/joc.3413, 2013.

445 Amante, C. and Eakins, B. W.: ETOPO1 Global Relief Model converted to PanMap layer format, https://doi.org/10.1594/PANGAEA.769615, 2009.

Barsugli, J. J., Ray, A. J., Livneh, B., Dewes, C. F., Heldmyer, A., Rangwala, I., Guinotte, J. M., and Torbit, S.: Projections of Mountain Snowpack Loss for Wolverine Denning Elevations in the Rocky Mountains, Earth's Future, 8, e2020EF001537, https://doi.org/https://doi.org/10.1029/2020EF001537, e2020EF001537 2020EF001537, 2020.

450 Beniston, M.: Climatic Change in Mountain Regions: A Review of Possible Impacts, Climatic Change, 59, 5–31, https://doi.org/10.1023/A:1024458411589, 2003.

Berghuijs, W. R., Woods, R. A., and Hrachowitz, M.: A precipitation shift from snow towards rain leads to a decrease in streamflow, Nature Climate Change, 4, 583–586, https://doi.org/10.1038/nclimate2246, 2014.

Birkeland, K. and Green, E.: Accurately Assessing Avalanche Size: The Ins and Outs of the R- and D-Scales, The Avalanche Review, 29, 455 27–28, https://avalanche.org/wp-content/uploads/2018/08/11_TAR_BirkelandGreene.pdf, 2011.

Boer, G. J.: Changes in Interannual Variability and Decadal Potential Predictability under Global Warming, Journal of Climate, 22, 3098–3109, https://doi.org/10.1175/2008JCLI2835.1, 2009.

Broxton, P., Zeng, X., and Dawson, N.: Daily 4 km Gridded SWE and Snow Depth from Assimilated In-Situ and Modeled Data over the Conterminous US, Version 1. Boulder, Colorado USA. NASA National Snow and Ice Data Center Distributed Active Archive Center. 460 1982–2017, Accessed April 2020, https://doi.org/https://doi.org/10.5067/0GGPB220EX6A, 2019.

Cooper, M. G., Nolin, A. W., and Safeeq, M.: Testing the recent snow drought as an analog for climate warming sensitivity of Cascades snowpacks, Environmental Research Letters, 11, 084 009, https://doi.org/10.1088/1748-9326/11/8/084009, 2016.

Crowley, N., Doolittle, C., King, J., Mace, R., and Seifer, J.: Drought and Outdoor Recreation: Impacts, Adaptation Strategies, and Information Gaps in the Intermountain West, NIDIS Drought Report, pp. 1–89, 2019.

465 Daly, C., Halbleib, M., Smith, J. I., Gibson, W. P., Doggett, M. K., Taylor, G. H., Curtis, J., and Pasteris, P. P.: Physiographically sensitive mapping of climatological temperature and precipitation across the conterminous United States, International Journal of Climatology, 28, 2031–2064, https://doi.org/10.1002/joc.1688, 2008.

Dierauer, J. R., Allen, D. M., and Whitfield, P. H.: Snow Drought Risk and Susceptibility in the Western United States and Southwestern Canada, Water Resources Research, 55, 3076–3091, https://doi.org/https://doi.org/10.1029/2018WR023229, 2019.

470 Evan, A. and Eisenman, I.: A mechanism for regional variations in snowpack melt under rising temperature, Nature Climate Change, https://doi.org/10.1038/s41558-021-00996-w, 2021.

Fisher, J. B., Melton, F., Middleton, E., Hain, C., Anderson, M., Allen, R., McCabe, M. F., Hook, S., Baldocchi, D., Townsend, P. A., Kilic, A., Tu, K., Miralles, D. D., Perret, J., Lagouarde, J.-P., Waliser, D., Purdy, A. J., French, A., Schimel, D., Famiglietti, J. S., Stephens, G., and Wood, E. F.: The future of evapotranspiration: Global requirements for ecosystem functioning, carbon and climate feedbacks, agricultural 475 management, and water resources, Water Resources Research, 53, 2618–2626, https://doi.org/https://doi.org/10.1002/2016WR020175, 2017.

Gibson, P. B., Waliser, D. E., Guan, B., DeFlorio, M. J., Ralph, F. M., and Swain, D. L.: Ridging Associated with Drought across the Western and Southwestern United States: Characteristics, Trends, and Predictability Sources, Journal of Climate, 33, 2485–2508, https://doi.org/10.1175/JCLI-D-19-0439.1, 2020.

480 Groisman, P. Y., Karl, T. R., and Knight, R. W.: Observed Impact of Snow Cover on the Heat Balance and the Rise of Continental Spring Temperatures, Science, 263, 198–200, https://doi.org/10.1126/science.263.5144.198, 1994.

Guan, B., Molotch, N. P., Waliser, D. E., Fetzer, E. J., and Neiman, P. J.: Extreme snowfall events linked to atmospheric rivers and surface air temperature via satellite measurements, Geophysical Research Letters, 37, https://doi.org/https://doi.org/10.1029/2010GL044696, 2010.

Hagenstad, M., Burakowski, E., and Hill, R.: The economic contributions of winter sports in a changing climate, Technical Report, 2018.

485 Hamed, K. H. and Rao, A. R.: A modified Mann-Kendall trend test for autocorrelated data, Journal of Hydrology, 204, 182–196, 1998.

Harpold, A., Dettinger, M., and Rajagopal, S.: Defining snow drought and why it matters, Eos, 98, EOS, 98, 2017.

Harpold, A. A. and Brooks, P. D.: Humidity determines snowpack ablation under a warming climate, Proceedings of the National Academy of Sciences, 115, 1215–1220, https://doi.org/10.1073/pnas.1716789115, 2018.

Hatchett, B. J.: Snow Level Characteristics and Impacts of a Spring Typhoon-Originating Atmospheric River in the Sierra Nevada, USA,
490 Atmosphere, 9, 233, https://doi.org/10.3390/atmos9060233, 2018.

Hatchett, B. J.: Seasonal and Ephemeral Snowpacks of the Conterminous United States, Hydrology, p. 2020110545, https://doi.org/10.20944/preprints202011.0545.v1, 2021.

Hatchett, B. J. and Eisen, H. G.: Brief Communication: Early season snowpack loss and implications for oversnow vehicle recreation travel planning, The Cryosphere, 13, 21–28, https://doi.org/10.5194/tc-13-21-2019, 2019.

495 Hatchett, B. J. and McEvoy, D. J.: Exploring the Origins of Snow Drought in the Northern Sierra Nevada, California, Earth Interactions, 22, 1–13, https://doi.org/10.1175/EI-D-17-0027.1, 2018.

Hatchett, B. J., Boyle, D. P., Garner, C. B., Kaplan, M. L., Putnam, A. E., and Bassett, S. D.: Magnitude and frequency of wet years under a megadrought climate in the western Great Basin, USA, Quaternary Science Reviews, 152, 197–202, https://doi.org/https://doi.org/10.1016/j.quascirev.2016.09.017, 2016.

500 Hatchett, B. J., Daudert, B., Garner, C. B., Oakley, N. S., Putnam, A. E., and White, A. B.: Winter Snow Level Rise in the Northern Sierra Nevada from 2008 to 2017, Water, 9, 2017.

Hatchett, B. J., Cao, Q., Dawson, P. B., Ellis, C. J., Hecht, C. W., Kawzenuk, B., Lancaster, J. T., Osborne, T. C., Wilson, A. M., Anderson, M. L., Dettinger, M. D., Kalansky, J. F., Kaplan, M. L., Lettenmaier, D. P., Oakley, N. S., Ralph, F. M., Reynolds, D. W., White, A. B., Sierks, M., and Sumargo, E.: Observations of an Extreme Atmospheric River Storm With a Diverse Sensor Network, Earth and Space
505 Science, 7, e2020EA001 129, https://doi.org/https://doi.org/10.1029/2020EA001129, e2020EA001129 2020EA001129, 2020.

Henn, B., Musselman, K. N., Lestak, L., Ralph, F. M., and Molotch, N. P.: Extreme Runoff Generation From Atmospheric River Driven Snowmelt During the 2017 Oroville Dam Spillways Incident, Geophysical Research Letters, 47, e2020GL088 189, https://doi.org/https://doi.org/10.1029/2020GL088189, e2020GL088189 2020GL088189, 2020.

Hossain, F., Arnold, J., Beighley, E., Brown, C., Burian, S., Chen, J., Mitra, A., Niyogi, D., Pielke, Sr., R., Tidwell, V., and Wegner, D.: What
510 Do Experienced Water Managers Think of Water Resources of Our Nation and Its Management Infrastructure?, PLOS ONE, 10, 1–10, https://doi.org/10.1371/journal.pone.0142073, 2015.

Huang, X., Hall, A. D., and Berg, N.: Anthropogenic Warming Impacts on Today's Sierra Nevada Snowpack and Flood Risk, Geophysical Research Letters, 45, 6215–6222, https://doi.org/https://doi.org/10.1029/2018GL077432, 2018.

Huning, L. S. and AghaKouchak, A.: Global snow drought hot spots and characteristics, Proceedings of the National Academy of Sciences, 117, 19 753–19 759, https://doi.org/10.1073/pnas.1915921117, 2020a.

Huning, L. S. and AghaKouchak, A.: Approaching 80 years of snow water equivalent information by merging different data streams, Scientific Data, 7, 333, https://doi.org/10.1038/s41597-020-00649-1, 2020b.

Huning, L. S., Margulis, S. A., Guan, B., Waliser, D. E., and Neiman, P. J.: Implications of Detection Methods on Characterizing Atmospheric River Contribution to Seasonal Snowfall Across Sierra Nevada, USA, Geophysical Research Letters, 44, 10,445–10,453, https://doi.org/https://doi.org/10.1002/2017GL075201, 2017.

Immerzeel, W. W., Lutz, A. F., Andrade, M., Bahl, A., Biemans, H., Bolch, T., Hyde, S., Brumby, S., Davies, B. J., Elmore, A. C., Emmer, A., Feng, M., Fernández, A., Haritashya, U., Kargel, J. S., Koppes, M., Kraaijenbrink, P. D. A., Kulkarni, A. V., Mayewski, P. A., Nepal, S., Pacheco, P., Painter, T. H., Pellicciotti, F., Rajaram, H., Rupper, S., Sinisalo, A., Shrestha, A. B., Viviroli, D., Wada, Y., Xiao, C., Yao, T., and Baillie, J. E. M.: Importance and vulnerability of the world's water towers, Nature, 577, 364–369, https://doi.org/10.1038/s41586-019-1822-y, 2020.

Jacobs, K. L. and Street, R. B.: The next generation of climate services, Climate Services, 20, 100 199, 2020.

Jennings, K. S., Winchell, T. S., Livneh, B., and Molotch, N. P.: Spatial variation of the rain–snow temperature threshold across the Northern Hemisphere, Nature Communications, 9, 1148, https://doi.org/10.1038/s41467-018-03629-7, 2018.

Kapnick, S. and Hall, A.: Causes of recent changes in western North American snowpack, Climate Dynamics, 38, 1885–1899, https://doi.org/10.1007/s00382-011-1089-y, 2012.

Klos, P. Z., Link, T. E., and Abatzoglou, J. T.: Extent of the rain-snow transition zone in the western U.S. under historic and projected climate, Geophysical Research Letters, 41, 4560–4568, https://doi.org/https://doi.org/10.1002/2014GL060500, 2014.

Livneh, B. and Badger, A. M.: Drought less predictable under declining future snowpack, Nature Climate Change, 10, 452–458, https://doi.org/10.1038/s41558-020-0754-8, 2020.

Livneh, B., Bohn, T. J., Pierce, D. W., Munoz-Arriola, F., Nijssen, B., Vose, R., Cayan, D. R., and Brekke, L.: A spatially comprehensive, hydrometeorological data set for Mexico, the U.S., and Southern Canada 1950–2013, Scientific Data, 2, 150 042, https://doi.org/10.1038/sdata.2015.42, 2015.

Luković, J., Chiang, J. C. H., Blagojević, D., and Sekulić, A.: A later onset of the rainy season in California, Geophysical Research Letters, n/a, e2020GL09 350, https://doi.org/https://doi.org/10.1029/2020GL090350, e2020GL09350 2020GL090350, 2021.

Lund, J., Medellin-Azuara, J., Durand, J., and Stone, K.: Lessons from California’s 2012–2016 Drought, Journal of Water Resources Planning and Management, 144, 04018 067, https://doi.org/10.1061/(ASCE)WR.1943-5452.0000984, 2018.

Lundquist, J. D., Neiman, P. J., Martner, B., White, A. B., Gottas, D. J., and Ralph, F. M.: Rain versus Snow in the Sierra Nevada, California: Comparing Doppler Profiling Radar and Surface Observations of Melting Level, Journal of Hydrometeorology, 9, 194–211, 2008.

Lynn, E., Cuthbertson, A., He, M., Vasquez, J. P., Anderson, M., Abatzoglou, J. T., and Hatchett, B. J.: Technical note: Precipitation-phase partitioning at landscape scales to regional scales, Hydrology and Earth Systems Science, Accepted, https://doi.org/https://doi.org/10.5194/hess-24-1-2020, 2020.

Margulis, S. A., Cortés, G., Girotto, M., and Durand, M.: A Landsat-Era Sierra Nevada Snow Reanalysis (1985–2015), Journal of Hydrometeorology, 17, 1203–1221, https://doi.org/10.1175/JHM-D-15-0177.1, 2016.

Margulis, S. A., Liu, Y., and Baldo, E.: A Joint Landsat- and MODIS-Based Reanalysis Approach for Midlatitude Montane Seasonal Snow Characterization, Frontiers in Earth Science, 7, 272, https://doi.org/10.3389/feart.2019.00272, 2019.

Marshall, A. M., Abatzoglou, J. T., Link, T. E., and Tennant, C. J.: Projected Changes in Interannual Variability of Peak Snowpack Amount and Timing in the Western United States, Geophysical Research Letters, 46, 8882–8892, https://doi.org/https://doi.org/10.1029/2019GL083770, 2019.

Marshall, A. M., Foard, M., Cooper, C. M., Edwards, P., Hirsch, S. L., Russell, M., and Link, T. E.: Climate change literature and information gaps in mountainous headwaters of the Columbia River Basin, Regional Environmental Change, 20, 134, https://doi.org/10.1007/s10113-020-01721-7, 2020.

McCabe, G. J., Clark, M. P., and Hay, L. E.: Rain-on-Snow Events in the Western United States, Bulletin of the American Meteorological Society, 88, 319–328, https://doi.org/10.1175/BAMS-88-3-319, 2007.

Mote, P. W., Li, S., Lettenmaier, D. P., Xiao, M., and Engel, R.: Dramatic declines in snowpack in the western US, npj Climate and Atmospheric Science, 1, 2, https://doi.org/10.1038/s41612-018-0012-1, 2018.

Musselman, K. N., Clark, M. P., Liu, C., Ikeda, K., and Rasmussen, R.: Slower snowmelt in a warmer world, Nature Climate Change, 7, 214–219, https://doi.org/10.1038/nclimate3225, 2017.

Musselman, K. N., Lehner, F., Ikeda, K., Clark, M. P., Prein, A. F., Liu, C., Barlage, M., and Rasmussen, R.: Projected increases and shifts in rain-on-snow flood risk over western North America, Nature Climate Change, 8, 808–812, https://doi.org/10.1038/s41558-018-0236-4, 2018.

Musselman, K. N., Addor, N., Vano, J. A., and Molotch, N. P.: Winter melt trends portend widespread declines in snow water resources, Nature Climate Change, 11, 418–424, https://doi.org/10.1038/s41558-021-01014-9, 2021.

Nolin, A. W. and Daly, C.: Mapping "At Risk" Snow in the Pacific Northwest, Journal of Hydrometeorology, 7, 1164–1171, https://doi.org/10.1175/JHM543.1, 2006.

Nolte, D. D.: The tangled tale of phase space, Physics Today, 63, 33–38, https://doi.org/10.1063/1.3397041, 2010.

O'Hara, B. F., Kaplan, M. L., and Underwood, S. J.: Synoptic Climatological Analyses of Extreme Snowfalls in the Sierra Nevada, Weather and Forecasting, 24, 1610–1624, https://doi.org/10.1175/2009WAF2222249.1, 2009.

Pendergrass, A. G., Knutti, R., Lehner, F., Deser, C., and Sanderson, B. M.: Precipitation variability increases in a warmer climate, Scientific Reports, 7, 17 966, https://doi.org/10.1038/s41598-017-17966-y, 2017.

Pepin, N., Bradley, R. S., Diaz, H. F., Baraer, M., Caceres, E. B., Forsythe, N., Fowler, H., Greenwood, G., Hashmi, M. Z., Liu, X. D., Miller, J. R., Ning, L., Ohmura, A., Palazzi, E., Rangwala, I., Schöner, W., Severskiy, I., Shahgedanova, M., Wang, M. B., Williamson, S. N., Yang, D. Q., and Group, M. R. I. E. W.: Elevation-dependent warming in mountain regions of the world, Nature Climate Change, 5, 424–430, https://doi.org/10.1038/nclimate2563, 2015.

Petersky, R. and Harpold, A.: Now you see it, now you don't: a case study of ephemeral snowpacks and soil moisture response in the Great Basin, USA, Hydrology and Earth System Sciences, 22, 4891–4906, https://doi.org/10.5194/hess-22-4891-2018, 2018.

Poff, N. L., Allan, J. D., Bain, M. B., Karr, J. R., Prestegaard, K. L., Richter, B. D., Sparks, R. E., and Stromberg, J. C.: The Natural Flow Regime, BioScience, 47, 769–784, 1997.

Qin, Y., Abatzoglou, J. T., Siebert, S., Huning, L. S., AghaKouchak, A., Mankin, J. S., Hong, C., Tong, D., Davis, S. J., and Mueller, N. D.: Agricultural risks from changing snowmelt, Nature Climate Change, 10, 459–465, https://doi.org/10.1038/s41558-020-0746-8, 2020.

Rhoades, A. M., Jones, A. D., and Ullrich, P. A.: Assessing Mountains as Natural Reservoirs With a Multimetric Framework, Earth's Future, 6, 1221–1241, https://doi.org/10.1002/2017EF000789, 2018a.

Rhoades, A. M., Jones, A. D., and Ullrich, P. A.: The Changing Character of the California Sierra Nevada as a Natural Reservoir, Geophysical Research Letters, 45, 13,008–13,019, https://doi.org/https://doi.org/10.1029/2018GL080308, 2018b.

Rhoades, A. M., Ullrich, P. A., and Zarzycki, C. M.: Projecting 21st century snowpack trends in western USA mountains using variable-resolution CESM, Climate Dynamics, 50, 261–288, https://doi.org/10.1007/s00382-017-3606-0, 2018c.

Scott, D.: Global Environmental Change and Mountain Tourism, chap. 3, p. 54–75, Routledge, London, https://doi.org/10.4324/9780203011911, 2006.

Seaber, P., Kapinos, F., and Knapp, G.: Hydrologic Unit Maps, U.S. Geological Survey Water-Supply Paper 2294, pp. 1–66, https://doi.org/https://doi.org/10.1016/S0034-4257(02)00098-6, 1987.

Serreze, M. C., Clark, M. P., Armstrong, R. L., McGinnis, D. A., and Pulwarty, R. S.: Characteristics of the western United States snowpack from snowpack telemetry (SNOTEL) data, Water Resources Research, 35, 2145–2160, https://doi.org/https://doi.org/10.1029/1999WR900090, 1999.

Siirila-Woodburn, E., Rhoades, A., Hatchett, B., Huning, L., Szinai, J., Tague, C., Nico, P., Feldman, D., Jones, A., Collins, W., and Kaatz, L.: Evidence of a low-to-no snow future and its impacts on water resources in the western United States, Nature Reviews Earth and Environment, Accepted, 2021.

Skiles, S. and Painter, T. H.: A nine-year record of dust on snow in the Colorado River Basin, in: Proceedings of the 12th Biennial Conference of Research on the Colorado River Plateau, edited by Ralston, B., pp. 1–128, U.S. Geological Survey Scientific Investigations Report 2015–5180, https://doi.org/10.3133/sir20155180, 2016.

Skiles, S. M., Flanner, M., Cook, J. M., Dumont, M., and Painter, T. H.: Radiative forcing by light-absorbing particles in snow, Nature Climate Change, 8, 964–971, https://doi.org/10.1038/s41558-018-0296-5, 2018.

Sterle, K., Hatchett, B. J., Singletary, L., and Pohll, G.: Hydroclimate Variability in Snow-Fed River Systems: Local Water Managers' Perspectives on Adapting to the New Normal, Bulletin of the American Meteorological Society, 100, 1031–1048, https://doi.org/10.1175/BAMS-D-18-0031.1, 2019.

Stieglitz, M., Déry, S. J., Romanovsky, V. E., and Osterkamp, T. E.: The role of snow cover in the warming of arctic permafrost, Geophysical Research Letters, 30, https://doi.org/https://doi.org/10.1029/2003GL017337, 2003.

Sturm, M., Goldstein, M. A., and Parr, C.: Water and life from snow: A trillion dollar science question, Water Resources Research, 53, 3534–3544, https://doi.org/https://doi.org/10.1002/2017WR020840, 2017.

Sumargo, E. and Cayan, D. R.: The Influence of Cloudiness on Hydrologic Fluctuations in the Mountains of the Western United States, Water Resources Research, 54, 8478–8499, https://doi.org/https://doi.org/10.1029/2018WR022687, 2018.

Svoboda, M., LeComte, D., Hayes, M., Heim, R., Gleason, K., Angel, J., Rippey, B., Tinker, R., Palecki, M., Stooksbury, D., Miskus, D., and Stephens, S.: THE DROUGHT MONITOR, Bulletin of the American Meteorological Society, 83, 1181–1190, https://doi.org/10.1175/1520-0477-83.8.1181, 2002.

Trujillo, E. and Molotch, N. P.: Snowpack regimes of the Western United States, Water Resources Research, 50, 5611–5623, https://doi.org/https://doi.org/10.1002/2013WR014753, 2014.

Ullrich, P. A., Xu, Z., Rhoades, A., Dettinger, M., Mount, J., Jones, A., and Vahmani, P.: California's Drought of the Future: A Midcentury Recreation of the Exceptional Conditions of 2012–2017, Earth's Future, 6, 1568–1587, https://doi.org/10.1029/2018EF001007, 2018.

Viviroli, D., Dürr, H. H., Messerli, B., Meybeck, M., and Weingartner, R.: Mountains of the world, water towers for humanity: Typology, mapping, and global significance, Water Resources Research, 43, https://doi.org/https://doi.org/10.1029/2006WR005653, 2007.

Wheeler, M. C. and Hendon, H. H.: An All-Season Real-Time Multivariate MJO Index: Development of an Index for Monitoring and Prediction, Monthly Weather Review, 132, 1917–1932, https://doi.org/10.1175/1520-0493(2004)132<1917:AARMMI>2.0.CO;2, 2004.

Xu, Y., Jones, A., and Rhoades, A.: A quantitative method to decompose SWE differences between regional climate models and reanalysis datasets, Scientific Reports, 9, 16 520, https://doi.org/10.1038/s41598-019-52880-5, 2019.

Yan, H., Sun, N., Wigmosta, M., Skaggs, R., Hou, Z., and Leung, R.: Next-Generation Intensity-Duration-Frequency Curves for Hydrologic Design in Snow-Dominated Environments, Water Resources Research, 54, 1093–1108, https://doi.org/https://doi.org/10.1002/2017WR021290, 2018.

Yarnell, S. M., Stein, E. D., Webb, J. A., Grantham, T., Lusardi, R. A., Zimmerman, J., Peek, R. A., Lane, B. A., Howard, J., and Sandoval-Solis, S.: A functional flows approach to selecting ecologically relevant flow metrics for environmental flow applications, River Research and Applications, 36, 318–324, https://doi.org/https://doi.org/10.1002/rra.3575, 2020.

Zeng, X., Broxton, P., and Dawson, N.: Snowpack Change From 1982 to 2016 Over Conterminous United States, Geophysical Research Letters, 45, 12,940–12,947, https://doi.org/10.1029/2018GL079621, 2018.